WATER RESOURCES RESEARCH, VOL. 49, 2424–2436, doi:10.1002/wrcr.20174, 2013

Transport and fate of microorganisms in soils with preferential flow under different solution chemistry conditions

Yusong Wang,[1] Scott A. Bradford,[2] and Jiří Šimůnek[1]

Received 25 June 2012; revised 14 February 2013; accepted 27 February 2013; published 17 May 2013.

[1] Laboratory and numerical studies were conducted to investigate the transport and fate of *Escherichia coli* D21g and coliphage φX174 in saturated soils with preferential flow under different solution ionic strength (IS = 1, 5, 20, and 100 m*M*) conditions. Preferential flow systems were created by embedding a coarse-sand lens (710 μm) into a finer matrix sand (120 μm). Complementary transport experiments were conducted in homogeneous sand columns to identify controlling transport and retention processes, and to independently determine model parameters for numerical simulations in the heterogeneous experiments. Results from homogeneous and heterogeneous transport experiments demonstrate that retention of *E. coli* D21g and φX174 increased with IS, while the effect on *E. coli* D21g in finer sand was much greater than in coarse sand. This microbe transport behavior was well described by numerical simulations. The importance of preferential flow on microbe transport was found to be enhanced at higher IS, even though the overall transport decreased. However, the contribution of preferential flow was much higher for *E. coli* D21g than φX174. Deposition profiles revealed significant cell retention at the interface of the coarse-sand lens and the fine-sand matrix as a result of mass transfer. Cell release from the preferential flow system with a reduction of solution IS exhibited multipulse breakthrough behavior that was strongly dependent on the initial amount of cell retention, especially at the lens-matrix interface.

Citation: Wang, Y., S. A. Bradford, and J. Šimůnek (2013), Transport and fate of microorganisms in soils with preferential flow under different solution chemistry conditions, *Water Resour. Res.*, *49*, 2424–2436, doi:10.1002/wrcr.20174.

1. Introduction

[2] Waterborne disease outbreaks associated with drinking water in the United States during 1971–2002 are known to have resulted in 575,457 cases of illness and 79 deaths, with 14% caused by bacteria, 19% by protozoa, 8% by viral pathogens, and 47% by unknown acute gastrointestinal illness [*Reynolds et al*., 2008]. Wastes from humans, domesticated and wild animals, birds, and insects frequently contain high concentrations of pathogenic microorganisms [*U.S. Department of Agriculture*, 1992; *U.S. Environmental Protection Agency*, 1998; *Gerba and Smith*, 2005] that serve as pathogen sources in agricultural settings. Pathogenic microorganisms can be transported to streams by surface water runoff and to ground water by recharge through the vadose zone. These contaminated surface and ground water supplies may eventually serve as drinking water and/or irrigation water for fresh produce. If these contaminated water supplies are not adequately treated before use, ground water typically receives minimal or no treatment, then they can put the public's health at risk.

[3] Much research has examined physical (size of the microbe and the porous medium, microbe concentration, water velocity, water content, and surface roughness) and chemical (surface chemistry of the microbe and soil, and aqueous solution pH, ionic strength (IS), and chemical composition) factors that influence the retention of microorganisms in homogeneous porous media under relatively uniform flow [*Mills et al*., 1994; *Mccaulou et al*., 1995; *Hendry et al*., 1999; *Yee et al*., 2000; *Dong et al*., 2002; *Bradford et al*., 2006b; *Chen and Walker*, 2007]. Mechanisms of microbe retention have been inferred from repacked column breakthrough curves (BTCs) and retention profiles (RPs), batch experiments, and complimentary micromodel studies that allowed for direct microscopic observation [*Ochiai et al*., 2006]. The mechanisms governing transport and retention of microbes in porous media have been described by several review articles [*Stevik et al*., 2004; *Sen and Khilar*, 2006; *Bradford and Torkzaban*, 2008].

[4] Field, lysimeter, and undisturbed soil column experiments have frequently revealed that microorganisms, colloids, and other contaminants can travel much deeper and faster than would be predicted based on results from laboratory studies in homogeneous porous media [*Bales et al*., 1989; *Abu-Ashour et al*., 1994; *Pivets and Steenhuis*, 1995; *Pivetz et al*., 1996; *Jiang et al*., 2010]. This phenomenon has been ascribed to transport in preferential flow pathways created by plant roots, burrowing earthworms [*Beven and*

[1]Department of Environmental Sciences, University of California, Riverside, California, USA.
[2]U.S. Salinity Laboratory, USDA, ARS, Riverside, California, USA.

Corresponding author: Y. Wang, Department of Environmental Sciences, University of California, Riverside, CA 92521, USA. (Ywang032@ucr.edu)

0043-1397/13/10.1002/wrcr.20174

Germann, 1982; *Madsen and Alexander*, 1982; *Unc and Goss*, 2003; *Cey et al*., 2009], and/or natural structural heterogeneities [*Wollum and Cassel*, 1978]. Preferential flow can also occur in soils and aquifers with strong contrasts in hydraulic conductivity between sediment layers [*Harvey et al*., 1993]. Considerable research has indicated that colloids and microorganisms can be transported in preferential flow pathways [*McGechan and Lewis*, 2002; *Jarvis*, 2007; *Pang et al*., 2008; *Cey et al*., 2009; *Cey and Rudolph*, 2009; *Passmore et al*., 2010]. Preferential flow has also been implicated in the rapid transport of bacteria to field tile drains [*Evans and Owens*, 1972; *Dean and Foran*, 1992; *Guzman et al*., 2009]. However, most of this research is qualitative in nature because of difficulty in quantifying the physical and chemical complexities of the soil matrix and macropore system with regard to microbe transport. This gap in information currently presents a great obstacle to predicting the fate of microbes in natural environments [*McCarthy and McKay*, 2004].

[5] The exchange rate of water between the macropore and the matrix, or between layers with contrasting hydraulic conductivities, will likely be a critical factor in determining the rate of microbe migration in preferential flow systems [*Harvey et al*., 1993; *Morley et al*., 1998; *Allaire-Leung et al*., 2000a, 2000b; *Allaire et al*., 2002a, 2002b] because of the potential for greater retention of microbes in the matrix as a result of enhanced chemical interactions, lower hydrodynamic forces, and smaller pore spaces. It is also possible that microbes may be physically excluded from the matrix, and in this case transport of microbes would exclusively occur in macropores. Optimum conditions for microbe transport in preferential flow systems will therefore likely depend on a wide variety of chemical and physical factors of both the matrix and macropore domains, but little quantitative research has addressed this issue, and the relative importance of these factors has not yet been fully determined [*Fontes et al*., 1991].

[6] It is important to be able to describe water flow in the preferential flow domain in order to quantitatively simulate the transport of microorganisms in the field. Various conceptual models of preferential flow exist that are dependent on a great number of parameters (e.g., macropore hydraulic properties, mass transfer terms, and macropore geometry) [*Šimůnek and van Genuchten*, 2008]. It is difficult, if not impossible, to independently determine all of the required model parameters under natural conditions [*Šimůnek et al*., 2003]. Thus, some assumptions have to be made to simplify the preferential flow path for simulation purposes. Artificial macropores can be systematically created by leaving small cylindrical openings in repacked columns [*Pivetz and Steenhuis*, 1995; *Castiglione et al*., 2003] or by packing different sized sands to generate layers and/or lens with contrasting hydraulic conductivities [*Fontes et al*., 1991; *Saiers et al*., 1994; *Morley et al*., 1998; *Bradford et al*., 2004]. The study of preferential flow and transport through artificial macropores provides an opportunity to overcome many modeling challenges, because the macropore geometry and hydraulic properties can be well defined and controlled in a repeatable manner [*Pivetz and Steenhuis*, 1995; *Castiglione et al*., 2003; *Guzman et al*., 2009; *Arora et al*., 2011, 2012]. Hence, it is possible to isolate and identify factors that have the greatest influence on preferential flow and transport in such systems. Furthermore, controlled preferential flow and transport studies provide valuable information on parameterization that is needed to help adapt numerical models to complex natural systems.

[7] Most studies of colloid and/or microbe transport through artificial macropores have focused on understanding the influence of physical heterogeneity on BTCs [*Fontes et al*., 1991; *Saiers et al*., 1994; *Morley et al*., 1998] and RPs [*Bradford et al*., 2004]. Numerical simulations of collected data demonstrate the importance of transverse mixing at the interface between the coarse-sand lens and the fine-sand matrix [*Saiers et al*., 1994; *Morley et al*., 1998] and the spatial distribution of retained colloids [*Bradford et al*., 2004]. Relatively little research has investigated the influence of microbe size and solution chemistry in preferential flow systems. *Fontes et al*. 1991 studied bacteria transport under two different IS conditions in a column with a coarse-sand lens imbedded in a finer soil matrix and demonstrated decreasing transport potential with an increase in IS. However, bacteria RPs were not determined in this study, and the data were not modeled. Furthermore, no published research has examined the release behavior of microbes with a reduction of solution IS in systems with artificial macropores. Consequently, our understanding of the effects of solution chemistry on microbe transport in preferential flow systems is still incomplete.

[8] The objective of this research was to study the coupled influence of physical and chemical factors on the transport of microorganisms in preferential flow systems. Transport experiments were conducted for two different sized microorganisms (*Escherichia coli* D21g and coliphage φX174) in packed columns with an artificial macropore at various IS conditions. Complementary transport experiments were also conducted with these microorganisms in homogeneously packed columns to independently determine many of the model parameters. RPs and the release of retained microorganisms after altering the IS of the soil solution were additionally studied for heterogeneous columns. Numerical simulation of the flow and transport behavior of the preferential flow system with HYDRUS (2D/3D) facilitated the quantification of flow and transport processes, especially the mass transfer and release behavior at the matrix/macropore interface.

2. Materials and Methods

2.1. Sands and Electrolyte Solutions

[9] Two sizes of Ottawa (quartz) sand were used in the column experiments described later. The median grain size (d_{50}) of these sands were 120 and 710 μm (referred to as fine sand and coarse sand later), and their corresponding coefficients of uniformity were equal to 1.6 and 1.3, respectively. A salt cleaning procedure was employed to remove kaolinite clay from the sand surfaces [*Bradford and Kim*, 2010] before use in the experiments to eliminate any background interference from clay particles.

[10] Electrolyte solutions that were used in column experiments consisted of autoclaved, deionized (DI) water with its pH 5.8 and the IS level adjusted to 0, 1, 5, 20, and 100 m*M* using NaCl or NaBr. These IS levels were selected to create a range of adhesive conditions between the

Table 1. Measured Zeta Potentials and Calculated Mean Interaction Energy Barrier Height and Depth of the Secondary Minima for *E. coli* D21g and φX174 on Approach to the Quartz Sand[a]

	Zeta Potential (mV)				Energy Barrier Height (kT)				Secondary Minima (kT)			
					E. coli D21g		φX174		*E. coli* D21g		φX174	
IS (m*M*)	Fine Sand	Coarse Sand	*E. coli* D21g	φX174	Fine Sand	Coarse Sand	Fine Sand	Coarse Sand	Fine Sand	Coarse Sand	Fine Sand	Coarse Sand
1	−80	−83	−60	−20	5520	5657	11.2	11.2	N/A	N/A	N/A	N/A
5	−81	−75	−52	−15	4317	4149	6.5	6.4	−0.5	−0.5	−0.01	−0.01
20	−80	−63	−43	−8.5	2920	2502	1.6	1.6	−2.6	−2.7	−0.03	−0.03
100	−40	−30	−13	−6.4	59	15.7	NB	NB	−23.4	−26.4	NB	NB

[a]NB, no energy barrier; N/A, not applicable.

microorganisms and sand. Bromide served as a conservative tracer in the column experiments. The effluent concentration of bromide was determined using a bromide-selective electrode (Thermo Scientific Orion bromide electrode ionplus® Sure-Flow®).

2.2. Microbes

[11] *E. coli* D21g and coliphage φX174 were selected as representative microorganisms for column transport experiments. *E. coli* D21g is a Gram-negative, nonmotile bacterial strain, which has minimal lipopolysaccharides, and negligible amounts of extracellular polymeric substances [*Walker et al*., 2004]. The effective diameter of *E. coli* D21g is 1.84 μm [*Walker et al*., 2004]. Coliphage φX174 is considered to be a conservative indicator for human virus transport. It is a spherical, single-stranded DNA coliphage with a 27 nm diameter and low hydrophobicity [*Dowd et al*., 1998].

[12] *E. coli* D21g was cultured in Luria-Bertani broth (LB broth, Fisher Scientific, Fair Lawn, NJ) containing 0.03 mg/L gentamycin (Sigma, St. Louis, MO) on a rotary shaker overnight (12–18 h) at 37°C. Then, 2 mL of liquid culture was transferred onto a LB media plate containing 0.03 mg/L gentamycin, and the plates were cultured overnight (12–18 h) at 37°C. Sterile water was placed on the plates, and the colonies were gently harvested using a sterile glass rod to release the colonies into solution. The bacteria suspension was then centrifuged to separate whole cells from the solution. The supernatant was decanted, and the bacteria were resuspended. These processes were repeated two times before diluting the concentrated suspension into the desired electrolyte solution to ensure that all traces of the growth medium were removed. A fresh cell suspension was prepared right before the start of each experiment. The concentrations of *E. coli* D21g in influent, effluent, and soil solution were determined using a spectrophotometer (Unico UV-200, United Products & Instruments, Dayton, NJ) at 600 nm [*Torkzaban et al*., 2008] and by the spread plating method [*Clesceri et al*., 1989] when necessary (e.g., low concentration).

[13] Coliphage φX174 was propagated at 37°C overnight on bacterial host *E. coli* CN-13 (ATCC 700609) at mid-exponential growth phase in Typtic soy broth supplemented with 1% nalixidic acid. The lysate was centrifuged (5000 × *g* for 20 min) and filtered (0.45 μm filter) to remove the cell debris and to recover the coliphage. The concentration of coliphage φX174 in aqueous solutions was determined using the double agar overlay method 1601 [*U.S. Environmental Protection Agency*, 2001] with bacterial host *E. coli* CN-13. The number of plaque forming units (pfu) was determined by counting the plaque density. All coliphage assays were run in duplicate and diluted as necessary.

[14] *E. coli* D21g and coliphage φX174 were added to the NaBr solutions to achieve influent concentrations (C_0) of approximately 1.0×10^8 cells/mL and approximately 1.0×10^7 pfu/mL, respectively. The suspension was continuously mixed during the column experiment using a magnetic stirrer. The values of C_0 for both microbes were measured three times during the course of a transport experiment to assess the reproducibility of the measurements and microbial survival. The spectrophotometer readings for *E. coli* D21g were within 1% of C_0, and the standard deviation of the spread plating method was 14.3% of C_0. The standard deviation of repeated measurements of φX174 was 13.1% of C_0. No systematic decrease in C_0 was observed over the duration of the column experiments, and this indicates that little inactivation occurred during this interval.

2.3. DLVO Calculations

[15] The zeta potential of coliphage φX174, *E. coli* D21g, and Ottawa sand crushed to a powder in various solution chemistries (Table 1) was calculated from experimentally measured electrophoretic mobilities using a ZetaPALS instrument (Brookhaven Instruments Corporation, Holtsville, NY) and the Smoluchowski equation. The total interaction energy of the φX174 and *E. coli* D21g upon approach to the Ottawa sand under the various solution chemistries was subsequently calculated (Table 1) using Derjaguin-Landau-Verwey-Overbeek (DLVO) theory and a sphere-plate assumption [*Verwey and Overbeek*, 1948; *Derjaguin*, 1954]. Electrostatic double-layer interactions were quantified using the expression of *Hogg et al*. 1966 using zeta potentials in place of surface potentials. The retarded London-van der Waals attractive interaction force was determined from the expression of *Gregory* 1981. Values of the Hamaker constant used in these calculations were 4×10^{-21} J [*Penrod et al*., 1996] and 6.5×10^{-21} J [*Rijnaarts et al*., 1995] for φX174 and *E. coli* D21g, respectively.

2.4. Homogeneous Column Experiments

[17] Glass chromatography columns (15 cm long and 4.8 cm inside diameter) were used in homogeneous transport experiments. A schematic of the experimental setup is given by *Bradford et al*. 2002. The columns were wet

Table 2. Experimental (Pore Water Velocity v) and Fitted Model (Bromide Dispersivity λ, Microbe Attachment Rate Coefficient k_{att}, and Maximum Solid Phase Concentration of Microbes, S_{max}) Parameters From the Homogeneous Fine- and Coarse-Sand Column Experiments With *E. coli* D21g and φX174 at Different Solution IS Conditions[a]

				E. coli D21g			φX174		
	IS (m*M*)	v (cm/min)	λ (cm)	k_{att}	S_{max}	R^2	k_{att}	S_{max}	R^2
Fine sand	1	0.33	0.10	0.0004	0.01	0.99	0.33	0.17	0.98
	5	0.31	0.10	0.066	1.1	0.99	ND	ND	ND
	20	0.34	0.13	0.2	3.5	0.95	ND	ND	ND
	100	0.37	0.14	0.48	4.8	0.99[b]	0.68[c]	0.16[c]	0.96
							0.034[d]	0.54[d]	
Coarse sand	20	10.3	0.52	0.001	0.1	1.00	ND	ND	ND
	100	10.3	0.59	0.005	0.4	0.97	ND	ND	ND

[a]The goodness of the model fit is quantified by the coefficient of linear regression (R^2) on breakthrough data unless otherwise noted. ND, not determined.
[b]Determined using RP information.
[c]Parameters for site 1.
[d]Parameters for site 2

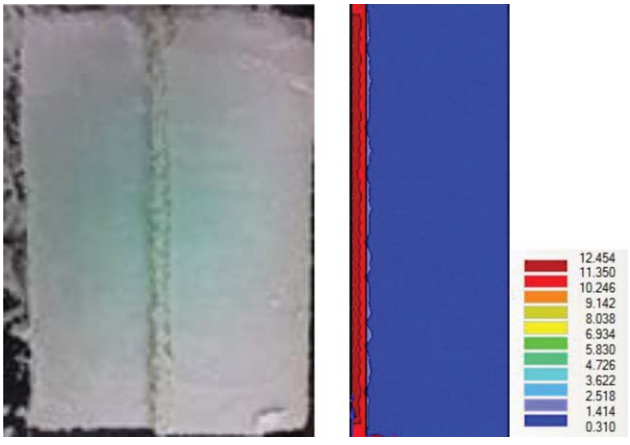

Figure 1. A representative picture of (left) heterogeneous column with lens in the center and (right) simulated flow field.

packed with a given size of Ottawa sand. The porosity of the packed columns was between 0.36 and 0.38, and the length of the columns was about 13 cm. Aqueous solutions were pumped upward through the vertically oriented columns at a steady flow rate using a peristaltic pump. The pore water velocities in the homogeneous column experiments (Table 2) were selected to be consistent with those measured in the heterogeneous column experiments described later.

[22] Two pore volumes (PVs) of a selected NaCl solution were flushed through a column, and the sand was allowed to equilibrate with this solution (phase 0) before initiating a microbial transport experiment. Microbial transport experiments were carried out in two phases. First, several PVs of microbe suspension and NaBr were introduced into the column at a constant rate and IS (phase 1). Second, NaCl solution was flushed through the column at the same flow rate and IS as in phase 1 until the effluent microbe concentration returned to a baseline level (phase 2). Effluent samples were continuously collected during the transport experiment at selected intervals using a fraction collector. The effluent samples were then analyzed for Br and microbe concentrations as described earlier. Replicate transport experiments were conducted for the different solution chemistry conditions.

[23] The microbial RPs in the sand of some columns were determined following completion of phases 1 and 2. The saturated sand was carefully excavated into tubes containing excess DI water. The tubes were shaken for 15 min to liberate any reversibly retained microbes, and the concentrations of *E. coli* D21g and coliphage φX174 in the excess solution were determined as described earlier. The volume of solution and mass of dry sand was determined from mass balance. The microbe mass recovery (%) was subsequently determined during phases 1 and 2 and for the RPs from mass balance and the injected amount (Table 3).

Table 3. Mass Balance Information (Effluent, Sand, and Total) for Homogeneous Fine- and Coarse-Sand Column Experiments With *E. coli* D21g and φX174 at Different Solution IS Conditions[a]

		Recovery (%)					
		E. coli D21g			φX174		
	IS (m*M*)	Effluent	Sand	Total	Effluent	Sand	Total
Fine sand	1	103	ND	103	69	1	70
	5	44	58	102	ND	ND	ND
	20	12	83	95	ND	ND	ND
	100	2	85	87	36	1	37
Coarse sand	20	98	3	101	ND	ND	ND
	100	92	12	104	ND	ND	ND

[a]ND, not determined.

2.5. Heterogeneous Column Experiments

[25] Heterogeneous column experiments were conducted in a plexiglass (acrylic) column, 22 cm long and 13.2 cm inside diameter. A polyester membrane (Saatifil PES 18/13) with an 18 μm nominal pore size was placed at the bottom of the column and connected to a hanging water column (tube) to control the bottom boundary pressure. Preferential flow systems were created by packing the fine (120 μm) and coarse (710 μm) sands into the column as follows: (i) the column was filled with autoclaved DI water to about one third of the column height, and a 30 cm long plastic tube with outside diameter of 1.14 cm was held in the center of the column; (ii) the fine sand was incrementally wet packed into the matrix portion of the column (outside the plastic tube) to a height of 20 cm; (iii) excess water in the plastic tube was drained from the bottom; (iv) the tube was carefully pulled out from the column without disturbing the surrounding fine matrix sand and leaving a 1.14 cm diameter hole in the center of the column; (v) the hole was then filled to a height of 20 cm with the coarse sand using a funnel to create a preferential flow lens; and (vi) the column was then saturated with water from the bottom. The porosity of the columns ranged from 0.34 to 0.36. Figure 1 shows an example of the artificial preferential flow path.

[26] Solutions were delivered onto the surface of the heterogeneous column at a steady flow rate using a rain

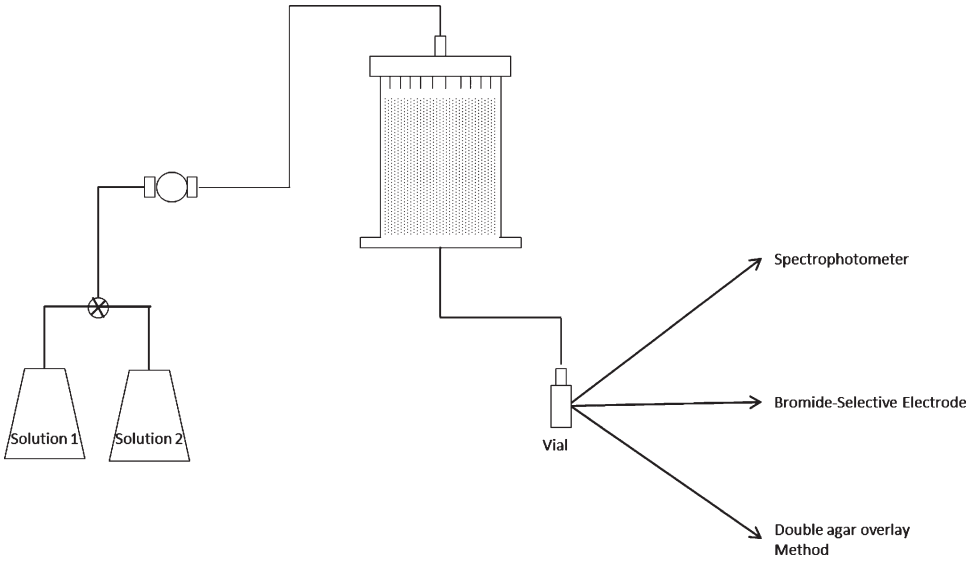

Figure 2. A schematic of the setup for transport experiments in heterogeneous columns.

simulator connected to a peristaltic pump. The water velocity was selected in order to just maintain saturated conditions (several millimeters of ponding at the surface) in the column through the experiments. Figure 2 shows a schematic of the experimental setup used for the preferential bromide and microbial transport experiments. Similar procedures were carried out to collect and analyze effluent samples in the homogeneous and heterogeneous column experiments. Furthermore, phases 0, 1, and 2 were conducted in an analogous fashion. After recovery of the BTCs, the distribution of retained microbes in the heterogeneous column was quantified as follows. Sand samples were taken at six equally spaced depths and three locations, namely, the lens, the matrix in the vicinity of the lens, and the bulk matrix. The determination of the amount of retained microbes in the sand was then determined in a similar manner to the homogeneous column experiments. Phases 1 and 2 of the heterogeneous column experiments were replicated for most solution chemistry conditions.

[27] Following recovery of the BTC for the microbes and bromide, some of the columns underwent an additional experimental phase 3 to determine the release of retained microbes with a reduction in solution IS. In this case, columns were flushed with autoclaved DI water at the same velocity as during phases 1 and 2 until the released microbe concentration in the effluent returned to a baseline level. The effluent samples were collected and analyzed using the same protocols as during phases 1 and 2.

[28] The saturated hydraulic conductivity (K_s) for the fine and coarse sands was directly measured to be 0.3 and 11 cm/min, respectively. However, the value of K_s in the matrix and lens was observed to vary somewhat for each heterogeneous column experiment due to small differences in packing and porosity. A more representative value of K_s for the matrix and lens was determined as follows. The value of K_s for the matrix was determined from the breakthrough time of the Br tracer from the matrix. The value of K_s for the lens was subsequently determined as the difference in the measured total flow rate and the matrix flow rate.

3. Numerical Modeling

[29] The HYDRUS-1D and HYDRUS (2D/3D) [Šimůnek *et al*., 2008] codes were used to simulate the transport of bromide and microbes in the homogeneous and heterogeneous column experiments, respectively. The HYDRUS codes simulate water flow using the Richards equation. Bromide transport was simulated using the advection-dispersion equation (ADE). Microbe transport and retention was simulated using the ADE with first-order terms for kinetic retention and release as shown later for the 2-D case:

$$\frac{\partial(\theta C)}{\partial t} = \frac{\partial}{\partial x_i}\left(\theta D_{ij}\frac{\partial C}{\partial x_j}\right) - \frac{\partial q_i C}{\partial x_i} - \theta\psi k_{\text{att}} C + \rho k_{\text{det}} S \qquad (1)$$

$$\frac{\partial(\rho S)}{\partial t} = \theta\psi k_{\text{att}} C - \rho k_{\text{det}} S, \qquad (2)$$

where subscripts i and j denote coordinate directions, C [$N_c L^{-3}$; L and N_c denote the units of length and number of microbes, respectively] is the microbe concentration in the aqueous phase, S [$N_c M^{-1}$; M denotes units of mass of soil] is the microbe concentration on the solid phase, D_{ij} [$L^2 T^{-1}$] is the hydrodynamic dispersion coefficient, q_i [LT^{-1}] is the Darcy water velocity in i direction, k_{det} [T^{-1}] is the microbe detachment rate coefficient, k_{att} [T^{-1}] is the microbe attachment rate coefficient, θ is the water content, and ρ [ML^{-3}] is the bulk density. The parameter ψ accounts for time- and concentration-dependent blocking using a Langmuirian approach as [*Adamczyk et al*., 1994]:

$$\psi = 1 - \frac{S}{S_{\max}}, \qquad (3)$$

where $S_{\max}$ [$N_c M^{-1}$] is the maximum solid phase concentration of microbes. In the case of φX174 at solution IS = 100 mM, a similar two-site kinetic retention was employed.

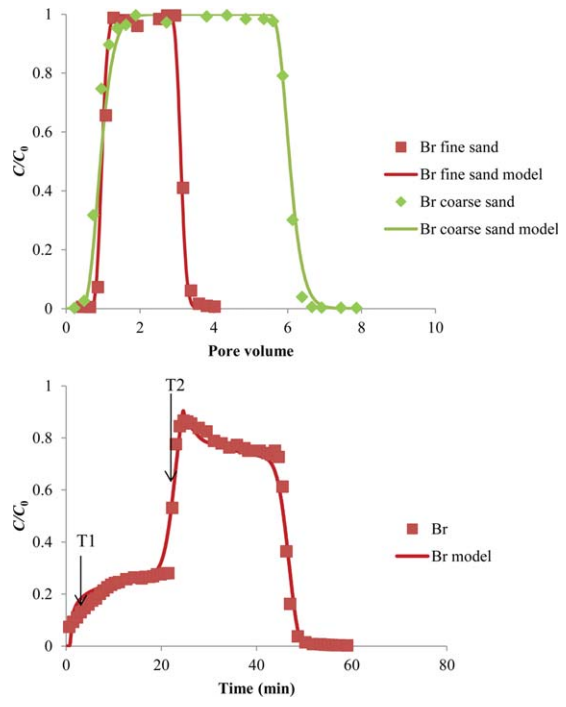

Figure 3. Representative plots of observed and simulated (model) normalized Br concentrations (C/C_0) in (top) homogeneous fine-sand and coarse-sand columns as a function of PV and (bottom) the heterogeneous column as a function of time. Parameter values are given in Tables 2 and 4.

[30] The homogeneous column transport experiments were simulated using a third-type boundary condition at the inlet and a zero concentration gradient at the outlet. The HYDRUS codes include a nonlinear least squares optimization routine to inversely estimate model parameters by fitting to experimental data. This option was used to determine Br and microbe transport parameters by fitting the experimental data from the homogeneous column experiments. In particular, the dispersivity was determined from the Br BTC, and the transport parameters (S_{max}, k_{att}, k_{det}) for microbes at given solution chemistry conditions were determined from measured microbe BTCs and/or RPs (Table 2).

[31] Bromide and microbe transport parameters obtained from the homogeneous column experiments were subsequently used in HYDRUS simulations of the heterogeneous column experiments with preferential flow. In this case, a 2-D axisymmetrical geometry was employed, and the model domain was 20 cm × 6.6 cm. This domain was subdivided into two vertical regions, with the left region representing the coarse lens in the center of the column with a radius of 0.57 cm and the remaining region representing the fine matrix sand. Domain discretization was designed to reduce simulation times while minimizing mass balance errors. A constant water flux boundary condition was employed at the soil surface, and a constant head was applied at the bottom boundary. A third-type boundary was chosen for the solute transport boundary condition at the inlet, and a zero concentration gradient was selected at the column outlet.

4. Results and Discussion

4.1. Bromide

[32] Representative plots of observed and simulated BTCs (C/C_0 versus PV) for the Br tracer in the homogeneous fine-sand and coarse-sand columns are shown in Figure 3. Bromide acted as a good conservative tracer, with good mass recovery and breakthrough at one PV. The 1-D ADE provided an excellent description of the homogeneous Br BTCs (Figure 3) when the dispersivity was inversely optimized to the data ($R^2 > 0.98$). Dispersivities were around 0.12 and 0.55 cm (Table 2) for fine- and coarse-sand columns, respectively.

[33] Figure 3 also provides representative observed and simulated BTCs for Br in a heterogeneous column that exhibited preferential flow. The very early breakthrough of Br (labeled as T1) demonstrated the extremely fast movement of water and solute through the artificial macropore. The peak value of C/C_0 in this first pulse was around 0.20–0.27, indicating that 20%–27% of the total water flux occurred through the macropore (Table 4). A second, higher ($C/C_0 = 0.83$–0.90) Br pulse (labeled as T2) occurred after about 22 min due to breakthrough of Br from the matrix material. The value of C/C_0 does not reach one for the matrix pulse because of the difference in arrival/ending times of the matrix and lens pulses; for example, the matrix pulse is diluted by NaCl solution from the lens. As mentioned earlier, the measured Br breakthrough times for the lens and matrix regions were used to refine estimates of the hydraulic properties in the heterogeneous column experiments. Table 2 provides a summary of the solute transport parameters that were used in subsequent HYDRUS simulations for each column. The values of the lens and matrix K_s (Table 4) and water fluxes (Table 4) were very consistent for the different column experiments, and this indicates that the artificial macropore was highly duplicable and had limited variation. Furthermore, the agreement between observed and simulated Br BTCs was very good ($R^2 > 0.92$ in Table 4). Simulations therefore provided an excellent description of water flow and Br transport in the heterogeneous systems.

4.2. *E. coli* D21g

[34] Figure 4 (top) presents observed and simulated BTCs for *E. coli* D21g in homogeneous fine sand when the solution IS equaled 1, 5, 20, and 100 m*M*. Figure 4 (bottom) gives similar information for the coarse sand when the

Table 4. Experimental Values of the Local (Lens and Matrix) Saturated Hydraulic Conductivity (K_s), the Percentage of Local Flux to Total Flux, and the Percentage of Local Transport to Total Transport in the Heterogeneous Column Experiments for *E. coli* D21g at Different Solution IS Conditions

	Lens			Matrix		
IS (m*M*)	K_s (cm/min)	Flux (%)	Transport (%)	K_s (cm/min)	Flux (%)	Transport (%)
1	11.2	25	26	0.31	75	74
5	11.8	27	38	0.31	73	62
20	10.5	27	68	0.31	73	32
100	10.6	20	99	0.33	80	1

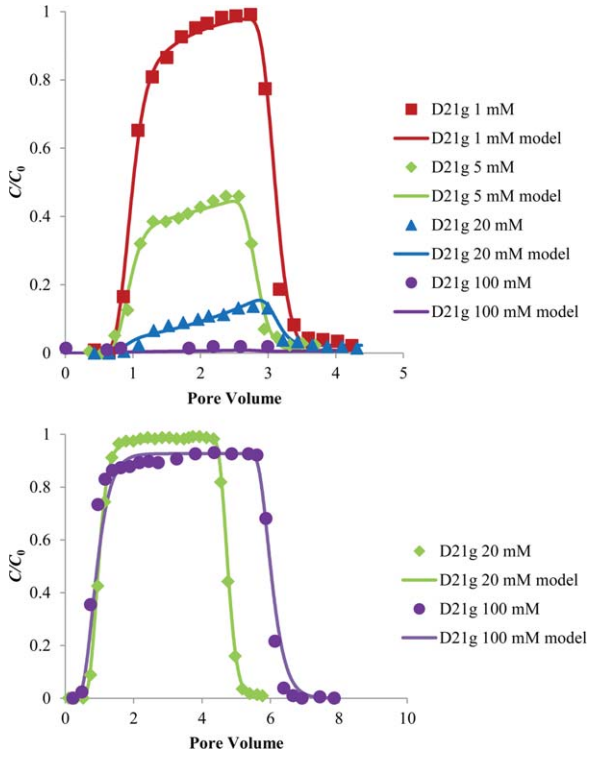

Figure 4. Observed and simulated (model) normalized effluent concentrations (C/C_0) of *E. coli* D21g as a function of PV in homogeneous (top) fine-sand and (bottom) coarse-sand columns at selected solution IS conditions. Parameter values are given in Table 2.

IS was 20 and 100 m*M*. Corresponding RPs and mass balance information for these systems are presented in Figure 5 and Table 3, respectively. RPs are plotted in Figure 5 as the normalized retained concentration of cells in the sand (S/C_0) as a function of the distance from the column inlet. Retention parameters (k_{att}, k_{det}, and S_{max}) were estimated by nonlinear least squares optimization to the experimental data (Table 2).

[35] Less breakthrough was observed for both fine sand and coarse sand as the IS increased (Figure 4). The effluent recovery rate for *E. coli* D21g decreased from 103% to 2% in the fine sand as the IS increased from 1 to 100 m*M* (Table 3). A similar trend occurred in the coarse sand, but changes in IS had a much less significant influence on the transport of *E. coli* D21g in coarse than in fine sand (Table 2). For example, when the IS = 100 m*M*, the recovery in the effluent was equal to 2% and 92% in the fine and coarse sands, respectively. Similar *E. coli* D21g transport experiments in the coarse sand were not conducted at IS = 1 and 5 m*M* because almost complete breakthrough occurred at IS = 20 and 100 m*M*. The RPs for *E. coli* D21g in the fine and coarse sand (Figure 5) followed complimentary trends to the BTCs shown in Figure 4, with increasing cell retention with IS and in the finer sand. The RPs tended to decrease exponentially with depth as predicted by the filtration theory [*Yao et al*., 1971].

[36] Simulations provided a good description of the *E. coli* D21g BTC and RP data ($R^2 > 0.95$ in Table 2), including the blocking behavior at intermediate IS conditions. Similar to experimental observations, the values of k_{att} and S_{max} increased with IS and were larger in the finer than the coarser sand (Table 2). The value of k_{det} was low in all cases; thus k_{det} was set as 0 for all simulations.

[37] A partial explanation for differences in the *E. coli* D21g transport behavior in coarse and fine sands is obtained from the filtration theory [*Yao et al*., 1971], which predicts that *E. coli* D21g mass transfer to the sand surface is greater for the finer than the coarser sand. Table 1 presents the calculated mean interaction energy height and depth of the secondary minimum for *E. coli* D21g on approach to the quartz sand. Unfavorable attachment conditions (i.e., the presence of a significant energy barrier in Table 1) are predicted to occur for all the solution IS. However, the depth of the secondary energy minimum increased with IS (Table 1) and followed a qualitatively similar trend to the amount of cell retention (Table 3).

[38] It should be mentioned that mean interaction energies do not reflect the potentially significant influence of microscopic heterogeneities on cell retention [*Duffadar and Davis*, 2008]. Evidence for the potential role of microscopic heterogeneities is obtained from the mass balance information (Table 3) and from fitted model parameters (Table 2). In particular, values of S_{max} increased with IS and in the finer sand (Table 2). Furthermore, the total mass

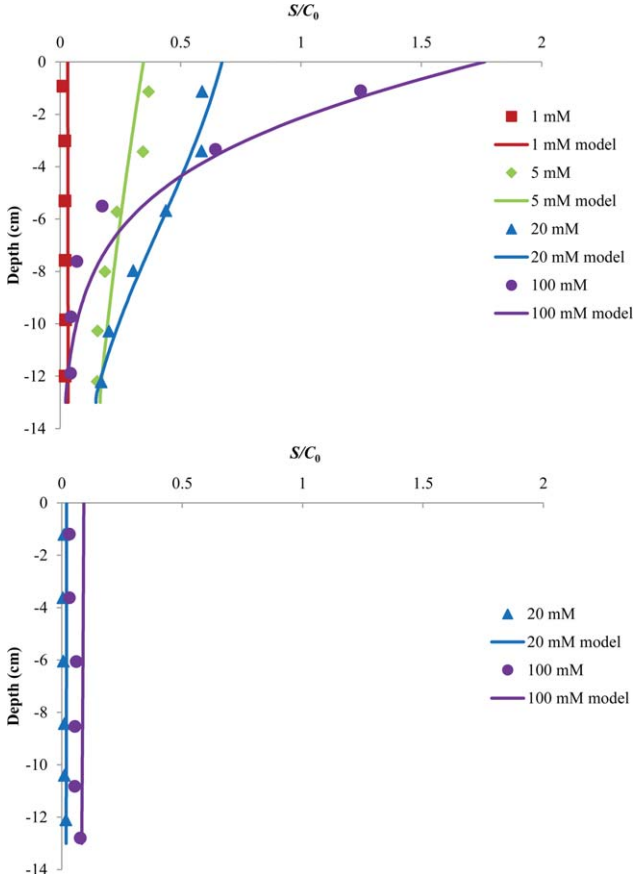

Figure 5. Observed and simulated (model) normalized solid phase concentrations (S/C_0) of *E. coli* D21g as a function of depth in homogeneous (top) fine-sand and (bottom) coarse-sand columns at selected solution IS conditions. Parameter values are given in Table 2.

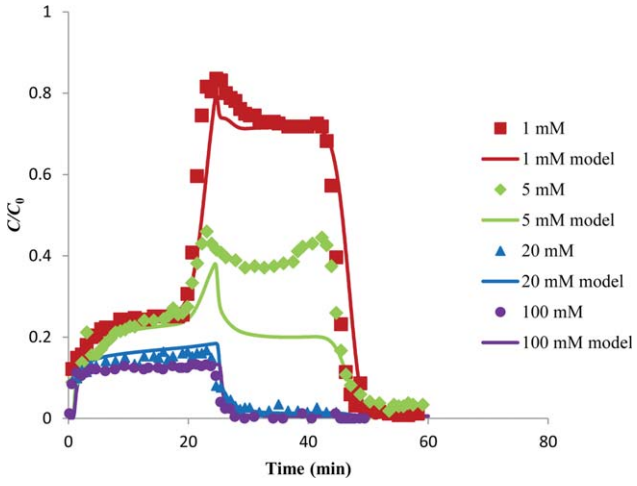

Figure 6. Observed and simulated (model) normalized effluent concentrations (C/C_0) of *E. coli* D21g as a function of time in heterogeneous columns at selected solution IS conditions. Parameter values are given in Tables 2 and 4.

recovery in the fine sand decreased from around 100% at IS = 1 m*M* to around 87% at IS = 100 m*M* (Table 3). This observation suggests that a small amount (<13%) of *E. coli* D21g was irreversibly retained (primary minimum) in the fine sand at IS = 100 m*M*. Conversely, mass balance information indicates that *E. coli* D21g reversibly interacted in a secondary minimum (>95%) at lower IS and in the coarse sand.

[39] Figure 6 presents observed and simulated BTCs for *E. coli* D21g in the heterogeneous columns when the solution IS equaled 1, 5, 20, and 100 m*M*. Corresponding mass balance information for these systems is presented in Table 5. Recall that the first pulse in the BTC is associated with transport through the lens, whereas the second pulse is controlled by the matrix. When the IS = 1 m*M* the effluent recovery of *E. coli* D21g was 96% (Table 5), and the BTCs for *E. coli* D21g (Figure 6) and Br (Figure 3) were very similar. However, the matrix breakthrough time for *E. coli* D21g was slightly earlier than for Br (21.5 compared to 23.0 min). This suggests that size exclusion may increases the transport velocity of *E. coli* D21g by constraining cells to faster flow domains and larger pore networks than Br [*Fontes et al*., 1991; *Ryan and Elimelech*, 1996; *Morley et al*., 1998; *Ginn*, 2002].

[41] Similar to homogeneous columns (Figure 4), the recovery of *E. coli* D21g in the effluent of the heterogeneous columns decreased from 96% to 13% (Table 5) as the solution IS increased from 1 to 100 m*M* (Figure 6). This trend is consistent with data presented by *Fontes et al*. 1991. The peak value of C/C_0 in the first pulse of the BTC for the lens decreased over a narrow range from 25% to 13% as the IS increased from 1 to 100 m*M*. In contrast, the peak value of C/C_0 in the second pulse of the BTC for the matrix decreased over a larger range from 77% to almost 0% as the IS increased from 1 to 100 m*M*. The contribution of preferential flow for the overall transport of *E. coli* D21g increased from 26% to 99% as IS changed from 1 to 100 m*M* (Table 4). This shows an interesting phenomenon that has not been reported by other researchers. Increasing the solution IS decreased the overall transport but increased the relative importance of preferential flow.

[42] Figure 7 shows the RPs for *E. coli* D21g in the lens, in the matrix adjacent to the lens, and in the bulk matrix sand when the IS = 100 m*M*. Similar to the homogeneous column experiments, greater amounts of *E. coli* D21g retention occurred in the matrix than the lens. Furthermore, the RPs in the lens and bulk matrix sands were quite similar to those observed in the corresponding homogeneous coarse- and fine-sand column experiments (Figure 5), respectively. The RPs of the matrix in the vicinity of lens provided strong evidence for the interaction between the lens and matrix sands. Simulation results presented by *Morley et al*. 1998 are consistent with this finding. In particular, retained concentrations of *E. coli* D21g in the matrix were higher next to the lens than in the bulk matrix at all depths. Deviation in the amount of *E. coli* D21g retention in the matrix adjacent to the lens and the bulk matrix was especially significant at depths greater than 6 cm. These observations demonstrate significant amounts of cell transport from the lens to the surrounding matrix and enhanced cell retention in the matrix than the lens.

[43] The transport and retention of *E. coli* D21g in the heterogeneous columns were again simulated using HYDRUS. Parameters values used in these simulations were obtained from corresponding Br data and *E. coli* D21g data in the homogeneous columns (Table 2). Longitudinal dispersivities of coarse and fine sands were set as the average values obtained from homogeneous experiments (0.55 cm and 0.12 cm) for all columns. Transverse dispersivity was set to be one tenth of the longitudinal dispersivity. The simulated BTCs (Figure 6) matched with the observed

Table 5. Experimental Mass Balance Information (Effluent During Phases 1 and 2, With DI Flush During Phase 3, and Total) for the Heterogeneous Column Experiments With *E. coli* D21g and φX174 Under Different Solution IS Conditions[a]

				Recovery (%)					
	R^2			*E. coli* D21g			φX174		
IS (m*M*)	Br	*E. coli* D21g	φX174	Effluent	DI	Total	Effluent	DI	Total
1	0.92	0.98	0.85	96	ND	96	98	ND	98
5	0.98	0.71	ND	61	32	93	ND	ND	ND
20	0.96	0.9	ND	32	61	93	ND	ND	ND
100	0.94	0.88	0.95	13	68	81	50	2	52

[a]The goodness of the model fit is also quantified by the coefficient of linear regression (R^2) on breakthrough data using model parameters in Tables 2 and 4. ND, not determined.

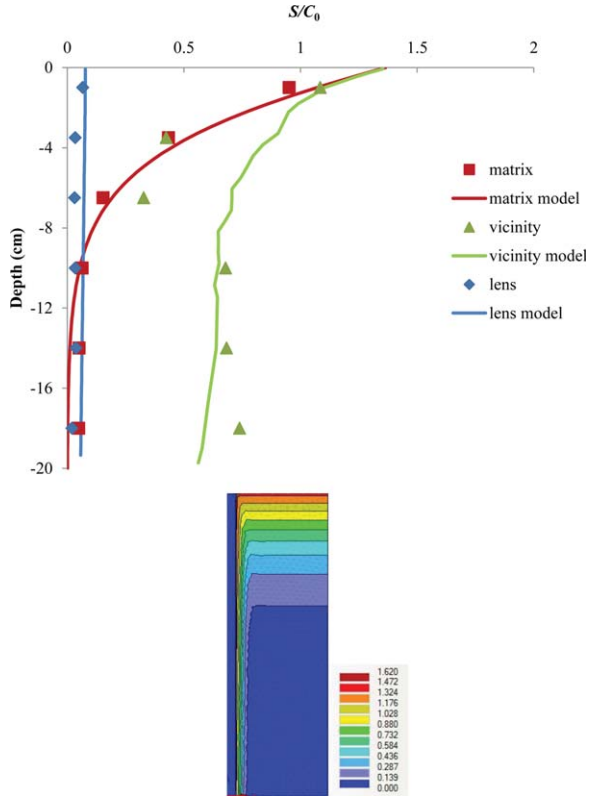

Figure 7. Observed and simulated (model) normalized solid phase concentrations (S/C_0) of *E. coli* D21g as (top) a function of depth in heterogeneous column at three different locations (lens, matrix in the vicinity of lens, and matrix) and (bottom) simulated spatial distribution of *E. coli* D21g in HYDRUS at solution IS = 100 m*M*. [Color figure can be viewed in the online issue, which is available at wileyonlinelibrary.com.]

BTCs reasonably well for all IS conditions ($R^2 > 0.71$ in Table 5). The simulations also provided a reasonable description of the measured RPs in the heterogeneous column (Figure 7). No significant water flow was observed at the interface of the lens and matrix in the simulation. Mass transfer at the lens-matrix interface was not very sensitive to the longitudinal dispersivity but was controlled by the transverse dispersivity and especially the concentration gradient.

[44] Additional experiments were conducted to better understand the significance of cell retention at the lens-matrix interface. In particular, after completion of phases 1 and 2 the heterogeneous columns were eluted with DI water (phase 3) to study cell release when the secondary minimum was eliminated. The release process was not simulated because of the coupling between cell retention parameters and variable IS. Figure 8 presents the release curves for *E. coli* D21g during phase 3. Similar to Figure 6, early breakthrough from the lens was observed just after switching to DI water. Release curves in homogeneous column experiments typically produce a sharp spike [*Bradford et al.*, 2007; *Torkzaban et al.*, 2010a]. In contrast, the first pulse of the release curve in the heterogeneous columns was more gradual and of a longer duration. This observation supports the above conclusion about the

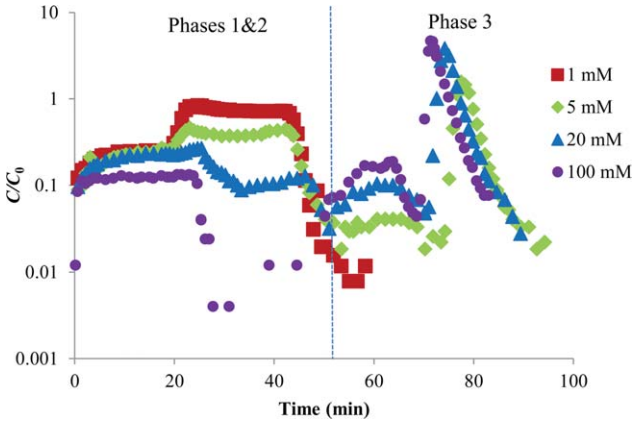

Figure 8. Semilog plots of observed normalized effluent concentrations (C/C_0) of *E. coli* D21g as a function of time in heterogeneous columns at selected solution IS conditions including phase 3.

interaction and mass transfer at the lens-matrix interface. A second sharp spike with extremely high cell concentrations came out from the matrix at about 22 min (consistent with the breakthrough time for the matrix). Greater release was obtained by flushing with DI water in systems with higher IS and greater cell retention during phases 1 and 2. The overall recovery rates of *E. coli* D21g (breakthrough and release) are provide in Table 5. Similar to the homogeneous columns, the overall recovery was lower than 100% and decreased with increasing IS.

4.3. Coliphage φX174

[45] Figure 9 presents observed and simulated BTCs for φX174 in homogeneous fine sand when the IS equaled 1 and 100 m*M*. In contrast to *E. coli* D21g, the BTCs for φX174 were slightly retarded, and the amount of retardation increased with IS. Similar behavior has been observed for other nanoparticles [*Torkzaban et al.*, 2010b]. The recovered φX174 in the column effluent was equal to 69% and 36% when the IS was 1 and 100 m*M*, respectively. The two-site kinetic model was selected for φX174 when IS = 100 m*M* for better performance. The transport simulation provided a good description of this data ($R^2 > 0.96$).

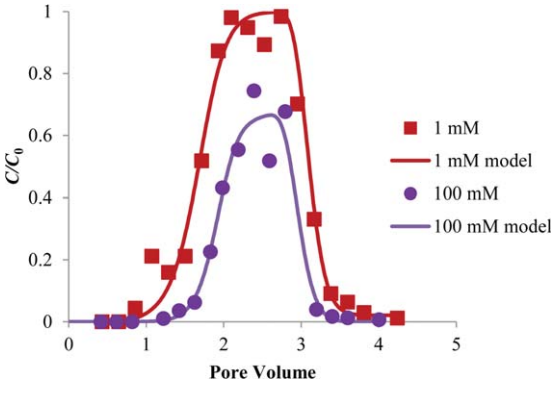

Figure 9. Observed and simulated (model) normalized effluent concentrations (C/C_0) of φX174 as a function of PV in homogeneous fine-sand columns at solution IS = 1 and 100 m*M*. Parameter values are given in Table 2.

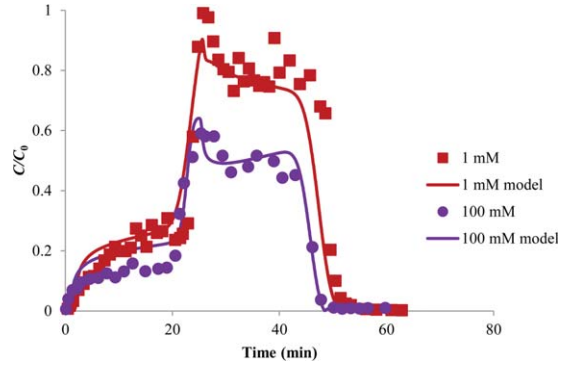

Figure 10. Observed and simulated (model) normalized effluent concentrations (C/C_0) of φX174 as a function of time in heterogeneous columns at solution IS = 1 and 100 m*M*. Parameter values are given in Tables 2 and 4. For the IS = 100 m*M* experiment the values of S_{max} were optimized to 0.04 and 0.15 for the two sites.

The parameter k_{det} was not needed to describe this data on a nonlog scale, suggesting mainly irreversible retention. Similarly, very small amounts of φX174 were recovered from the sand (<2%). The RPs for φX174 could therefore not be accurately determined. The effect of microscopic heterogeneities on colloid retention has been reported to increase, as the colloid size decreases [*Duffadar and Davis*, 2008]. These observations suggest that φX174 was subject to irreversible, primary minimum attachment to a larger extent than *E. coli* D21g.

[46] Retention of φX174 was less than *E. coli* D21g when the IS = 100 m*M*, but greater than *E. coli* D21g when the IS = 1 m*M*. These differences in the retention depend on the values of k_{att} and S_{max} given in Table 2. Filtration theory [*Yao et al*., 1971] predicts that k_{att} is proportional to the product of the colloid collector efficiency (η) and the sticking efficiency (α). The value of η was predicted [*Tufenkji and Elimelech*, 2003] to be much larger for φX174 ($\eta = 0.28$) than *E. coli* D21g ($\eta = 0.02$). Conversely, α and S_{max} depend in a complex manner on the depth of the secondary minimum and hydrodynamic forces [*Shen et al*., 2010], surface macromolecules [*Kim et al*., 2009], and physical and chemical heterogeneities [*Bendersky and Davis*, 2011]. Furthermore, the influence of the secondary minimum and chemical heterogeneity changes with IS and colloid size.

[47] Transport experiments for φX174 in the fine sand when the IS = 5 and 20 m*M* were not conducted because the expected differences in the BTCs (intermediate to 1 and 100 m*M* data shown in Figure 9) were within the analytic error. Similarly, φX174 retention in the coarse sand at IS equal to 1 and 100 m*M* was initially assumed to be zero because the *E. coli* D21g data (Figure 4) exhibited much less retention in the coarse than the fine sand for given IS conditions (Table 3). The validity of this assumption will be verified in the heterogeneous column experiments discussed later.

[48] Figure 10 presents BTCs for φX174 in heterogeneous columns when the IS equaled 1 and 100 m*M*. Chemistry had a very similar influence on the transport of φX174 as for *E. coli* D21g (Figure 6). In particular, the overall transport decreased with an increase in the IS, but the contribution of preferential flow increased. The recovery changed from 98% to 50% when the IS was 1 and 100 m*M*, respectively. The peak value of C/C_0 in the lens (first) and matrix (second) pulses changed from 28% to 18% and 99% to 58% when the IS was 1 and 100 m*M*, respectively. In contrast to *E. coli* D21g, higher values of C/C_0 were observed for φX174 at comparable IS conditions, and the contribution of preferential flow was much lower (26%–34% with an increase in IS). This observation suggests that φX174 is less influenced by physical heterogeneity than *E. coli* D21g and thereby behaves more similar to Br because of its smaller size.

[49] The simulation could not provide a good description of the φX174 data in the heterogeneous column when using parameter values from the homogeneous fine-sand column experiments. Large variations in C_0 and the degree of sand cleaning could cause significant difference in S_{max} for the fine sand in the homogeneous and heterogeneous column experiments. Therefore, we used the same values of k_{att} from the homogeneous fine-sand column and optimized separate values of S_{max} to the heterogeneous matrix data. Values of R^2 were greater than 0.85 with the optimized S_{max}.

[50] In contrast to *E. coli* D21g (Figure 8), only small amounts of φX174 were released from the lens and matrix during phase 3 when the IS was reduced from 100 m*M* to DI water. Similar to the minimal recovery of φX174 from the sand, this observation reflects that φX174 was mainly irreversibly retained in a primary minimum.

4.4. Limitations of the Mathematical Model

[51] It needs to be emphasized that the mathematical model used here to describe the transport and fate of microorganisms has its limitations with respect to the complexity of processes involved in the transport of microorganisms in soils, as well as with respect to modeling preferential transport. The model considers attachment/detachment as first-order processes and neglects other processes such as straining and/or size exclusion. Additionally, only Langmuirian-type blocking was considered, while other blocking models could have been used as well. Microbes were treated as having a uniform size distribution, and aggregation and other biological activities were not considered in the model. Note that the analysis of the effects of these various processes can be found elsewhere (e.g., *Bradford et al*. 2003 for straining and size exclusion; *Bradford et al*. 2006a for different blocking mechanisms; *Bradford et al*. 2005 for ripening behavior; *Bradford et al*. 2006b for cell aggregation; *Gargiulo et al*. 2006 for cell growth; and *Bradford et al*. 2006c for virus inactivation).

[52] It should also be stressed that application of our 2-D model for preferential flow in natural systems is difficult because it requires detailed information on the spatial distribution of soil hydraulic properties which produce preferential flow paths. To overcome this limitation, flow and transport in preferential pathways are sometimes described using a dual permeability model that divides flow into fast and slow regimes [e.g., *Jarvis*, 2007; *Šimůnek and van Genuchten*, 2008]. However, this approach is more common for variably saturated conditions than for fully saturated conditions.

5. Summary and Conclusions

[53] DLVO calculations indicate that the depth of the secondary minimum increased and that the height of the energy barrier deceased with an increase in IS. Consequently, retention of *E. coli* D21g and φX174 was enhanced as the solution IS increased in both homogeneous and heterogeneous sand columns. This effect of IS was found to be especially significant for *E. coli* D21g in the finer sand. In general, *E. coli* D21g was mainly reversibly retained in the sand as a result of interactions in a secondary minima, whereas φX174 was largely irreversible retained as a result of primary minima interactions. HYDRUS proved to be a powerful tool to simulate the transport and deposition behavior of *E. coli* D21g and φX174 in both homogenous and preferential flow systems under the different IS conditions.

[54] The relative amount of preferential transport of microbes through the lens increased with IS. This indicates that preferential transport of microbes became more important under conditions of higher overall retention. Cell RPs demonstrated significant amounts of mass transfer at the interface between the lens and matrix. Cell release with a reduction in solution IS exhibited multipeaked breakthrough in the preferential flow systems. The amount of cell release was sensitive to the initial distribution of retained cells, especially at the lens-matrix interface. Accurate predictions of microorganism transport and fate in fields with preferential flow and transients in solution chemistry require information on BTCs, RPs, and release behavior.

[55] The artificial macropore method proved to be a reliable and repeatable way to study transport processes in systems with preferential flow. Further study will be done to investigate the influence of macropore geometry with the artificial macropore method, which can help improve our understanding of natural environments. Numerical models still need to be improved to better characterize mass transfer at the matrix-lens interface and the release of microorganisms with transients in solution IS. Furthermore, alternative mathematical models are warranted to predict transport behavior in more complicated systems and at larger scales in order to connect the studies in idealized artificial macropore system with the real processes in natural systems.

[56] **Acknowledgments.** We would like to thank Lorena Altamirano for her help in conducting some of the experimental research presented herein. This research was supported in part by the USDA, ARS, NP 214, and Multistate Research Funded project W-2188. The USDA is an equal opportunity provider and employer.

References

Abu-Ashour, J., D. M. Joy, H. Lee, H. R. Whiteley, and S. Zelin (1994), Transport of microorganisms through soil, *Water Air Soil Pollut.*, *75*, 141–158.

Adamczyk, Z., B. Siwek, M. Zembala, and P. Belouschek (1994), Kinetics of localized adsorption of colloid particles, *Adv. Colloid Interface*, *48*, 151–280, doi:10.1016/0001–8686(94)80008-1.

Allaire, S. E., S. C. Gupta, J. Nieber, and J. F. Moncrief (2002a), Role of macropore continuity and tortuosity on solute transport in soils: 2. Interactions with model assumptions for macropore description, *J. Contam. Hydrol.*, *58*(3–4), 283–298.

Allaire, S. E., S. C. Gupta, J. Nieber, and J. F. Moncrief (2002b), Role of macropore continuity and tortuosity on solute transport in soils: 1. Effects of initial and boundary conditions, *J. Contam. Hydrol.*, *58*(3–4), 299–321.

Allaire-Leung, S. E., S. C. Gupta, and J. F. Moncrief (2000a), Water and solute movement in soil as influenced by macropore characteristics: 1. Macropore continuity, *J. Contam. Hydrol.*, *41*(3–4), 283–301.

Allaire-Leung, S. E., S. C. Gupta, and J. F. Moncrief (2000b), Water and solute movement in soil as influenced by macropore characteristics: 2. Macropore tortuosity, *J. Contam. Hydrol.*, *41*(3–4), 303–315.

Arora, B., B. P. Mohanty, and J. T. McGuire (2011), Inverse estimation of parameters for multidomain flow models in soil columns with different macropore densities, *Water Resour. Res.*, *47*, W04512, doi:10.1029/2010WR009451.

Arora, B., B. P. Mohanty, and J. T. McGuire (2012), Uncertainty in dual permeability model parameters for structured soils, *Water Resour. Res.*, *48*, W01524, doi:10.1029/2011WR010500.

Bales, R. C., C. P. Gerba, G. H. Grondin, and S. L. Jensen (1989), Bacteriophage transport in sandy soil and fractured tuff, *Appl. Environ. Microbiol.*, *55*(8), 2061–2067.

Bendersky, M., and J. M. Davis (2011), DLVO interaction of colloidal particles with topographically and chemically heterogeneous surfaces, *J. Colloid Interface Sci.*, *353*(1), 87–97, doi:10.1016/j.jcis.2010.09.058.

Beven, K., and P. Germann (1982), Macropores and water-flow in soils, *Water Resour. Res.*, *18*(5), 1311–1325.

Bradford, S. A., and H. Kim (2010), Implications of cation exchange on clay release and colloid-facilitated transport in porous media, *J. Environ. Qual.*, *39*(6), 2040–2046, doi:10.2134/Jeq2010.0156.

Bradford, S. A., and S. Torkzaban (2008), Colloid transport and retention in unsaturated porous media: A review of interface-, collector-, and pore-scale processes and models, *Vadose Zone J.*, *7*(2), 667–681.

Bradford, S. A., S. R. Yates, M. Bettahar, and J. Šimůnek (2002), Physical factors affecting the transport and fate of colloids in saturated porous media, *Water Resour. Res.*, *38*(12), 1327, doi:10.1029/2002WR001340.

Bradford, S. A., J. Šimůnek, M. Bettahar, M. Th. van Genuchten, and S. R. Yates (2003), Modeling colloid attachment, straining, and exclusion in saturated porous media, *Environ. Sci. Technol.*, *37*, 2242–2250.

Bradford, S. A., M. Bettehar, J. Šimůnek, and M. Th. van Genuchten (2004), Straining and attachment of colloids in physically heterogeneous porous media, *Vadose Zone J.*, *3*(2), 384–394.

Bradford, S. A., M. Th. van Genuchten, and J. Šimůnek (2005), Modeling *of colloid transport and deposition in porous media, in* Workshop on HYDRUS: Advanced Modeling of Water Flow and Solute Transport in the Vadose Zone, pp. 1–5, Univ. of Utrecht, Utrecht, Netherlands, 17–19 Oct.

Bradford, S. A., J. Šimůnek, M. Bettahar, M. Th. van Genuchten, and S. R. Yates (2006a). Significance of straining in colloid deposition: Evidence and implications. *Water Resour. Res.*, *42*, W12S15, doi:10.1029/2005WR004791.

Bradford, S. A., J. Šimůnek, and S. L. Walker (2006b), Transport and straining of *E. coli* O157: H7 in saturated porous media, *Water Resour. Res.*, *42*, W12S12, doi:10.1029/2005WR004805.

Bradford, S. A., Y. F. Tadassa, and Y. Jin (2006c), Transport of coliphage in the presence and absence of manure suspension, *J. Environ. Qual.*, *35*, 1692–1701.

Bradford, S. A., S. Torkzaban, and S. L. Walker (2007), Coupling of physical and chemical mechanisms of colloid straining in saturated porous media, *Water Res.*, *41*(13), 3012–3024, doi:10.1016/j.watres.2007.03.030.

Castiglione, P., B. P. Mohanty, P. J. Shouse, J. Šimůnek, M. T. van Genuchten, and A. Santini (2003), Lateral water diffusion in an artificial macroporous system, *Vadose Zone J.*, *2*(2), 212–221, doi:10.2113/2.2.212.

Cey, E. E., and D. L. Rudolph (2009), Field study of macropore flow processes using tension infiltration of a dye tracer in partially saturated soils, *Hydrol. Processes*, *23*(12), 1768–1779.

Cey, E. E., D. L. Rudolph, and J. Passmore (2009), Influence of macroporosity on preferential solute and colloid transport in unsaturated field soils, *J. Contam. Hydrol.*, *107*(1–2), 45–57.

Chen, G. X., and S. L. Walker (2007), Role of solution chemistry and ion valence on the adhesion kinetics of groundwater and marine bacteria, *Langmuir*, *23*(13), 7162–7169.

Clesceri, L. S., A. E. Greenberg, and R. R. Trussel (1989), *Standard Methods for the Examination of Water and Waste Water*, 17th ed., Am. Public Health Assoc., Washington, D. C.

Dean, D. M., and M. E. Foran (1992), The effect of farm liquid waste application on tile drainage, *J. Soil Water Conserv.*, *47*(5), 368–369.

Derjaguin, B. V. (1954), A theory of the heterocoagulation, interaction and adhesion of dissimilar particles in solutions of electrolytes, *Discus. Faraday Soc.*, *18*, 85–98.

Dong, H. L., T. C. Onstott, M. F. Deflaun, M. E. Fuller, T. D. Scheibe, S. H. Streger, R. K. Rothmel, and B. J. Mailloux (2002), Relative dominance of physical versus chemical effects on the transport of adhesion-deficient bacteria in intact cores from South Oyster, Virginia, *Environ. Sci. Technol.*, *36*(5), 891–900.

Dowd, S. E., S. D. Pillai, S. Y. Wang, and M. Y. Corapcioglu (1998), Delineating the specific influence of virus isoelectric point and size on virus adsorption and transport through sandy soils, *Appl. Environ. Microb.*, *64*(2), 405–410.

Duffadar, R. D., and J. M. Davis (2008), Dynamic adhesion behavior of micrometer-scale particles flowing over patchy surfaces with nanoscale electrostatic heterogeneity, *J. Colloid Interface Sci.*, *326*(1), 18–27, doi:10.1016/j.jcis.2008.07.004.

Evans, M. R., and J. D. Owens (1972), Factors affecting the concentration of faecal bacteria in land-drainage water, *J. Gen. Microbiol.*, *71*(3), 477–485, doi:10.1099/00221287-71-3–477.

Fontes, D. E., A. L. Mills, G. M. Hornberger and J. S. Herman (1991), Physical and chemical factors influencing transport of microorganisms through porous media, *Appl. Environ. Microbiol.*, *57*(9), 2473–2481.

Gargiulo, G., S. A. Bradford, J. Šimůnek, H. Vereecken, and E. Klumpp (2006), Transport and deposition of metabolically active and stationary phase *Deinococcus radiodurans* in unsaturated porous media, *Environ. Sci. Technol.*, *41*, 1265–1271.

Gerba, C. P., and J. E. Smith (2005), Sources of pathogenic microorganisms and their fate during land application of wastes, *J. Environ. Qual.*, *34*, 42–48, doi:10.2134/jeq2005.0042.

Ginn, T. R. (2002), A travel time approach to exclusion on transport in porous media, *Water Resour. Res.*, *38*(4), 1041, doi:10.1029/2001WR000865.

Gregory, J. (1981), Approximate expressions for retarded van der Waals interaction, *J. Colloid Interface Sci.*, *83*(1), 138–145, doi:10.1016/0021–9797(81)90018-7.

Guzman, J. A., G. A. Fox, R. W. Malone, and R. S. Kanwar (2009), *Escherichia coli* transport from surface-applied manure to subsurface drains through artificial biopores, *J. Environ. Qual.*, *38*, 2412–2421.

Harvey, R. W., N. E. Kinner, D. MacDonald, E. W. Metge, and A. Bunn (1993), Role of physical heterogeneity in the interpretation of small scale laboratory and field observations of bacteria, microbial-sized microsphere, and bromide transport through aquifer sediments, *Water Resour. Res.*, *29*(8), 2713–2721.

Hendry, M. J., J. R. Lawrence, and P. Maloszewski (1999), Effects of velocity on the transport of two bacteria through saturated sand, *Ground Water*, *37*(1), 103–112.

Hogg, R., T. W. Healy, and D. W. Fuerstenau (1966), Mutual coagulation of colloidal dispersions, *Trans. Faraday Soc.*, *62*, 1638–1651.

Jarvis, N. J. (2007), A review of non-equilibrium water flow and solute transport in soil macropores: Principles, controlling factors and consequences for water quality, *Eur. J. Soil. Sci.*, *58*(3), 523–546.

Jiang, S., L. Pang, G. D. Buchan, J. Šimůnek, M. J. Noonan, and M. E. Close (2010), Modeling water flow and bacterial transport in undisturbed lysimeters under irrigations of dairy shed effluent and water using HYDRUS-1D, *Water Res.*, *44*, 1050–1061, doi:10.1016/j.watres.2009.08.039 [special issue].

Kim, H. N., S. A. Bradford, and S. L. Walker (2009), *Escherichia coli* O157:H7 transport in saturated porous media: Role of solution chemistry and surface macromolecules, *Environ. Sci. Technol.*, *43*(12), 4340–4347, doi:10.1021/Es8026055.

Madsen, E. L., and M. Alexander (1982), Transport of *Rhizobium* and *Pseudomonas* through soil, *Soil Sci. Soc. Am. J.*, *46*(3), 557–560.

McCarthy, J. F., and L. D. McKay(2004), Colloid transport in the subsurface: Past, present, and future challenges, *Vadose Zone J.*, *3*, 326–337.

Mccaulou, D. R., R. C. Bales, and R. G. Arnold (1995), Effect of temperature-controlled motility on transport of bacteria and microspheres through saturated sediment, *Water Resour. Res.*, *31*(2), 271–280.

McGechan, M. B., and D. R. Lewis (2002), Transport of particulate and colloid-sorbed contaminants through soil. Part 1: General principles, *Biosyst. Eng.*, *83*(3), 255–273.

Mills, A. L., J. S. Herman, G. M. Hornberger, and T. H. Dejesus (1994), Effect of solution ionic-strength and iron coatings on mineral grains on the sorption of bacterial-cells to quartz sand, *Appl. Environ. Microb.*, *60*(9), 3300–3306.

Morley, L. M., G. M. Hornberger, A. L. Mills, and J. S. Herman (1998), Effects of transverse mixing on transport of bacteria through heterogeneous porous media, *Water Resour. Res.*, *34*(8), 1901–1908.

Ochiai, N., E. L. Kraft, and J. S. Selker (2006), Methods for colloid transport visualization in pore networks, *Water Resour. Res.*, *42*, W12S06, doi:10.1029/2006WR004961.

Pang, L., M. McLeod, J. Aislabie, J. Šimůnek, M. Close, and R. Hector (2008), Modeling transport of microbes in ten undisturbed soils under effluent irrigation, *Vadose Zone J.*, *7*(1), 97–111.

Passmore, J. M., D. L. Rudolph, M. M. F. Mesquita, E. E. Cey, and M. B. Emelko (2010), The utility of microspheres as surrogates for the transport of *E. coli* RS2g in partially saturated agricultural soil, *Water Res.*, *44*(4), 1235–1245.

Penrod, S. L., T. M. Olson, and S. B. Grant (1996), Deposition kinetics of two viruses in packed beds of quartz granular media, *Langmuir*, *12*(23), 5576–5587, doi:10.1021/la950884d.

Pivetz, B. E. and T. S. Steenhuis (1995), Soil matrix and macropore biodegradation of 2,4-D, *J. Environ. Qual.*, *24*, 564–570.

Pivetz, B. E., I. W. Kelsey, T. S. Steenhuis, and M. Alexander (1996), A procedure to calculate biodegradation during preferential flow through heterogeneous soil columns, *Soil Sci. Soc. Am. J.*, *60*, 381–388.

Reynolds, K. A., K. D. Mena, and C. P. Gerba (2008), Risk of waterborne illness via drinking water in the United States, *Rev. Environ. Contam. Toxicol.*, *192*, 117–158.

Rijnaarts, H. H. M., W. Norde, E. J. Bouwer, J. Lyklema, and A. J. B. Zehnder (1995), Reversibility and mechanism of bacterial adhesion, *Colloids Surf. B: Biointerfaces*, *4*(1), 5–22, doi:10.1016/0927–7765(94)01146-v.

Ryan, J. N., and M. Elimelech (1996), Colloid mobilization and transport in groundwater, *Colloids Surf. A*, *107*, 1–56.

Saiers, J. E., G. M. Hornberger, and C. Harvey (1994), Colloidal silica transport through structured, heterogeneous porous media, *J. Hydrol. (Amsterdam)*, *163*, 271–288.

Sen, T. K., and K. C. Khilar (2006), Review on subsurface colloids and colloid-associated contaminant transport in saturated porous media, *Adv. Colloid Interface*, *119*(2–3), 71–96.

Shen, C., Y. Huang, B. Li, and Y. Jin (2010), Predicting attachment efficiency of colloid deposition under unfavorable attachment conditions, *Water Resour. Res.*, *46*, W11526, doi:10.1029/2010WR009218.

Šimůnek, J., and M. Th. van Genuchten (2008), Modeling nonequilibrium flow and transport with HYDRUS, *Vadose Zone J.*, doi:10.2136/VZJ2007.0074 [special issue Vadose Zone Model., *7*(2), 782–797].

Šimůnek, J., N. J. Jarvis, M. T. van Genuchten, and A. Gardenas (2003), Review and comparison of models for describing non-equilibrium and preferential flow and transport in the vadose zone, *J. Hydrol.*, *272*, 14–35.

Šimůnek, J., M. T. van Genuchten, and M. Sejna (2008), Development and applications of the HYDRUS and STANMOD software packages and related codes, *Vadose Zone J.*, *7*(2), 587–600, doi:10.2136/Vzj2007.0077.

Stevik, T. K., K. Aa, G. Ausland, and J. F. Hanssen (2004), Retention and removal of pathogenic bacteria in wastewater percolating through porous media: A review, *Water Res.*, *38*(6), 1355–1367.

Torkzaban, S., S. S. Tazehkand, S. L. Walker, and S. A. Bradford (2008), Transport and fate of bacteria in porous media: Coupled effects of chemical conditions and pore space geometry, *Water Resour. Res.*, *44*, W04403, doi:10.1029/2007WR006541.

Torkzaban, S., H. N. Kim, J. Šimůnek, and S. A. Bradford (2010a), Hysteresis of colloid retention and release in saturated porous media during transients in solution chemistry, *Environ. Sci. Technol.*, *44*(5), 1662–1669, doi:10.1021/Es903277p.

Torkzaban, S., Y. Kim, M. Mulvihill, J. Wan, and T. K. Tokunaga (2010b), Transport and deposition of functionalized CdTe nanoparticles in saturated porous media, *J. Contamin. Hydrol.*, *118*, 208–217.

Tufenkji, N., and M. Elimelech (2003), Correlation equation for predicting single-collector efficiency in physicochemical filtration in saturated porous media, *Environ. Sci. Technol.*, *38*(2), 529–536, doi:10.1021/es034049r.

Unc, A., and M. J. Goss (2003), Movement of faecal bacteria through the vadose zone, *Water Air Soil Pollut.*, *149*(1–4), 327–337.

U.S. Department of Agriculture (1992), *National Engineering Handbook: Agricultural Waste Management Field Handbook*, Part 651 (210-AWMFH, 4/92), chap. 3, pp. 1–29, Washington, D. C.

U.S. Environmental Protection Agency (1998), *Environmental Impacts of Animal Feeding Operations, U.S. Environ. Prot. Agency, Off. of Water*, Stand. and Appl. Sci. Div., Washington, D. C.

U.S. Environmental Protection Agency (2001), *Method 1601: Male-specific (F+) and somatic coliphage in water by two-step enrichment procedure,* EPA-821-R-01–030*, U.S. Environ. Prot. Agency*, Off. of Water, Eng. and Anal. Div., Washington, D. C.

Verwey, E. J. W., and J. T. G. Overbeek (1948), *Theory of the Stability of Lyophobic Colloids*, Elsevier, Amsterdam.

Walker, S. L., J. A. Redman, and M. Elimelech (2004), Role of cell surface lipopolysaccharides in *Escherichia coli* K12 adhesion and transport, *Langmuir*, *20*(18), 7736–7746, doi:10.1021/La049511f.

Wollum, A. G., II, and D. K. Cassel (1978), Transport of microorganisms in sand columns. *Soil Sci. Soc. Am. J.*, *42*, 72–76.

Yao, K.-M., M. T. Habibian, and C. R. O'Melia (1971), Water and waste water filtration. Concepts and applications, *Environ. Sci. Technol.*, *5*(11), 1105–1112, doi:10.1021/es60058a005.

Yee, N., J. B. Fein, and C. J. Daughney (2000), Experimental study of the pH, ionic strength, and reversibility behavior of bacteria-mineral adsorption, *Geochim. Cosmochim. Acta*, *64*(4), 609–617.